

Transformations in Exposure to Debris Flows in Post-Earthquake Sichuan, China

Isabelle Utley¹, Tristram Hales¹, Ekbal Hussain², Xuanmei Fan³

[1] School of Earth and Environmental Sciences, Cardiff University, Cardiff, CF10 3AT, UK.

[2] British Geological Survey, Keyworth, Nottingham, NG12 5GG, UK

[3] State Key laboratory of Geohazard Prevention, Chengdu University of Technology, Chengdu, China

Correspondence to: Isabelle E.K Utley (ieku20@bath.ac.uk)

Abstract. Post-earthquake debris flows can exceed volumes of $1 \times 10^6 \text{ m}^3$ and pose significant challenges to downslope recovery zones. These stochastic hazards form when intense rain remobilises coseismic landslide material. As communities recover from earthquakes they mitigate the effects of these debris flows through modifications to catchments such as building check dams and levees. We investigate the relationship between how different catchment interventions changing change exposure and hazard of post-2008 debris flows in three gullies in Sichuan province, China. These were selected based on the number of post-earthquake check dams – Cutou (2), Chediguan (2) and Xiaojia (none). Using high resolution satellite images, we developed a multitemporal building inventory from 2005 to 2019, comparing it to spatial distribution of previous debris flows and future modelled events. Post-earthquake urban development in Cutou and Chediguan increased exposure to a major debris flow in 2019 with inundation impacting 40% and 7% of surveyed structures respectively. We simulated future debris flow runouts using LAHARZ to investigate the role of check dams in mitigating three flow volumes – 10^4 m^3 (low), 10^5 m^3 (high) and 10^6 m^3 (extreme). Our simulations show check dams effectively mitigate exposure to low and high flow events but prove ineffective for extreme events with 59% of buildings in Cutou, 22% in Chediguan and 33% in Xiaojia significantly affected. We verified our analyses through employing a statistical exposure model, adapted from a social vulnerability equation. Cutou's exposure increased by 64% in 2019, Chediguan's by 52% whilst only 2% for Xiaojia in 2011, highlighting that extensive grey infrastructure correlates with higher exposure to extreme debris flows, but less so to smaller events. Our work suggests the presence of check dams increases the perception of exposure reduction downstream, however, ultimately produces a levee effect that raises exposure to large events.

Keywords

Debris Flows, Built Environment, Exposure, Check dams, LAHARZ.

1. Introduction

Major earthquakes such as the 1994 M_w 6.8 event in Northridge, California (Harp and Jibson, 1996) and the 1999 M_w 7.3 earthquake in Chi-Chi, Taiwan (Liu et al., 2008) have triggered chains of hazards; that increase the exposure of local communities to secondary hazards for many years after the initial disaster. Following the 2008 M_w 7.9 Wenchuan earthquake in Sichuan, China, debris flows occurred more frequently and at a higher magnitude ($>1 \times 10^6 \text{ m}^3$) after the earthquake compared to flows before the earthquake (Cruden and Varnes., 1996; Cui et al., 2008; Huang and Li., 2009; Guo et al., 2016; Thouret et al., 2020). Increased debris flow frequency impacts vulnerable communities and local infrastructure, potentially reshaping the demographic and structural landscape of previously rural regions (Chen et al., 2011). The frequency of post-seismic flows is heavily influenced by sediment availability, which is often controlled by coseismic landslide distribution, hydrology, and slope (Horton et al., 2019). The ready transformation and remobilisation of seismically loosened deposits into water-laden sediments leads to a heightened probability of debris flow hazards for extended periods, further exacerbating the potential impacts felt by these areas (Costa et al., 1984; Huang & Li, 2014; Fan et al., 2019b).

Post-seismic debris flows affect the expanding built environment and communities located in the flat land that forms along floodplains and on debris and alluvial fans. In addition to direct loss of life, debris flows repeatedly block and/or destroy rivers, roads, tunnels, and bridges, and damage property and agriculture, and result in loss of life (Chen, N et al., 2011). Buildings are particularly highly susceptible to the impacts of debris flows (Hu et al., 2012; Zeng et al., 2015), with property damage accounting responsible for nearly all impacts such as i.e., casualties and fatalities (Wei et al., 2018; Wei et al., 2022). Variations in construction materials are a particularly important factor in determining structural resilience and vulnerability to debris flows (Zhang, S et al., 2018). Despite focus on building resilience and reducing vulnerability, post-earthquake regions are often areas of significant rebuilding and expansion of infrastructure so the exposure to debris flows changes rapidly in these areas. The

development of critical infrastructure such as highways and tunnels further encourages the growth of the built environment and subsequent influx of people settling in areas exposed to geological hazards (Cruden and Varnes, 1996; Jiang et al., 2016).

Check dams are a common form of risk mitigation for debris flows globally (Zeng et al., 2009; Peng et al., 2014; Cucchiaro, S. et al., 2019b), and one that is prevalent in post-earthquake Wenchuan (Chen, X. et al., 2015; Guo et al., 2016). Check dams store debris flow sediment, locally reduce channel slope, and are often permeable to affect debris flow hydrology. However, they have significant disadvantages such as requiring regular maintenance (to reduce sediment inputs) (Kean et al., 2018). The mitigation potential of these structures is contingent on their position along a channel, their height, amount of sediment fill, and their strength (which depends on the materials used for construction) (Dai et al., 2017). These factors evolve through time, meaning that the hazard-mitigating factor of check dams can varyies withthrough time and often with unpredictable results with unknown sign. The presence of check dams changes the downstream risk, primarily by altering through changing the magnitude and frequency distribution of debris flows within the channel. For well-made check dams of sufficient volume to mitigate the largest debris flows, this can reduce the downstream risk of debris flows to negligible by effectively mitigating the entire hazard. However, in the case of the Wenchuan region, check dams are rarely large enough or regularly cleared of sediment to mitigate the largest debris flows, which can exceed 10^6 m^3 in volume.

The presence of check dams, particularly in drainage basins with a limited history of catastrophic debris flow events, may affect the perception of risk downstream. They serve to stabilize, obstruct, drain, and/or halt the movement of flows (Hübl and Fiebigler, 2005; Chen et al., 2015). The perception that check dams have mitigated all hazards may promote the expansion of infrastructure into floodplains and debris fans, potentially increasing exposure to debris flows that overtop dams or occur due to dam failure. The increase of exposure is common on floodplains where the presence of flood control levees can promote building onto floodplains – a process known as the that is called the levee effect (Collenteur et al., 2015). In the flooding example, the presence of levees reduces the frequency of small and medium sized floods, but when large floods occur that cause those levees to fail, heightened floodplain exposure can lead to higher damage. The effect of check dams on risk perception is less well understood. Anecdotal examples from the Wenchuan region (e.g., Hongchun, Taoguan gullies) show that large debris flow events in 2010, 2013 and 2019 caused significant damage despite the presence of check dams (Dai et al., 2017). However, it is not clear if the presence of check dams affected exposure relative to the large-scale expansion of infrastructure in the post-earthquake recovery phase.

This study seeks to understand whether the addition of engineered mitigation measures, namely primarily, check dams, have influenced the susceptibility of post-earthquake Wenchuan communities to large-scale debris flows. We compare 3 catchments with similar topography and geology, but different levels of mitigation. We measure the building exposure of buildings to debris flow events in two neighbouring catchments with containing check dams (Cutou and Chediguan) using and compare with a third, unmitigated gully (Xiaojia) as a control measure. We examine how infrastructure develops in the basins with time and as a function of check dam measures. By analysing infrastructure development in these catchments, particularly in Cutou and Chediguan in the years following mitigation – will seek to assess how check dam construction has impacted infrastructure growth and compare the potential exposure to debris flow events of different sizes. Additionally, our analysis will explore whether the presence of these structures has impacted risk perception and/or land-use decisions in 'at-risk' catchments.

2. Study Area: Sichuan Province, China

China's mountainous regions, including the Longmenshan, account for 69% of the country's land mass with over a third of the population living in these regions (Chen et al., 2011; He et al., 2022). 72% of this landscape suffers from debris flow activity. Between 2005 and 2018, estimates suggest over 800 debris flow occurrences each year (He et al., 2022; Wei et al., 2021). Of these, landslides dominate provinces in the North and debris flows are generally constrained to provinces in the South (Liu et al., 2018). The 2008 Mw 7.9 Wenchuan earthquake primarily impacted Sichuan province (Fig 1). The epicentre was located near Yinxu, Wenchuan County, within the seismically active Longmenshan Fault Zone (Li et al., 2019). The shaking triggered around 56,000 landslides and displaced nearly 3 km^3 of loose material (Fan et al., 2018; Luo et al., 2020). In subsequent years, the unstable material has been reactivated as debris flows, many of which exceed 10^6 m^3 in mobilised volume (Frances et al., 2022). The risk from these debris flows has been compounded by increasing exposure due to China's rapid rural development programme, which includes the construction of roads, bridges, and industrial facilities (Tang et al., 2022).

Commented [IU1]: 4. The introduction and conclusion sections should better align with the research objectives. (RIC)

Four significant episodes of debris flows occurred in the post-earthquake Wenchuan region in 2008, 2010, 2013 and 2019 (Tang et al., 2022; Fan et al., 2019b). Each event was associated with monsoon rainfall that occurred in different parts of the range. The largest flow surges, containing millions of cubic meters of sediment were located in the gullies along the Minjiang in Sichuan. Large scale flooding further amplified the impacts, for example in Yingxiu Town, Wenchuan County (Liu et al., 2016b). Debris flow events occurring post-earthquake often exhibit larger material volumes compared to flow events recorded prior to 2008. Horton et al., (2019) attributed the increase in flow volume to ~~the large-scale high in channel sediment volumes that can drive bulking displacement of sediment during the earthquake.~~ The resulting increase in debris flow hazards necessitated; engineered mitigation measures to reduce risk levels in the basin communities (Tang et al., 2009; Huang et al., 2009; Huang, 2012).

In this study we focus on three gullies along the Minjiang - Cutou, Chediguan and Xiaojia and debris flow events on August 20th, 2019, and 4th July 2011 (Fig 1). Cumulative rainfall on 20th August 2019 peaked at 83 mm in Cutou and 65 mm in Chediguan resulting in large debris flows measuring over ~~50x10⁴ 50 × 10⁴~~ m³ in each gully. Cutou gully is known for its high frequency of post-seismic debris flows, which has been attributed to the total of 11x10⁶ m³ coseismic deposits generated by the earthquake (Yan et al 2014). Although a check dam was built in 2011 to manage debris flow impacts in Chediguan gully a large damaging debris flow of 64x10⁴ m³ occurred on 20 August 2019 and destroyed the drainage groove and G213 Taiping Middle Bridge (Li et al., 2021). The debris briefly blocked river flow in the Minjiang causing water levels to rise during flood peak. This led to flooding at the Taipingyi hydropower station located 200 m upstream.

Xiaojia gully, is a moderate debris flow hazard area based on limited past occurrences and has no existing engineered mitigation measures. Following a period of debris flow activity in 2010, and after a period of continuous heavy rainfall approximately 30,000m³ of deposits were remobilised and transported along the channel to the gully mouth. This event led to a period of disruption on the S303 road from flooding (Liu et al., 2014).

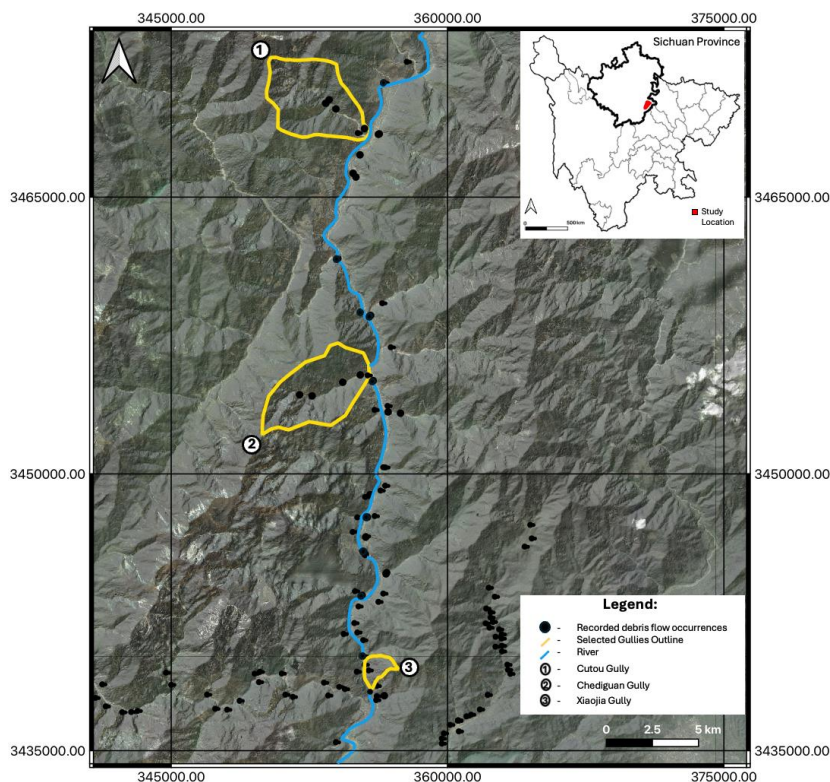


Figure 1: Location of the three gullies that form the focus of this study within Sichuan Province. Recorded post-2008 landslide occurrences are from the Wang et al. (2022) multitemporal datasets (© Google Earth 2019).

3. Methodology

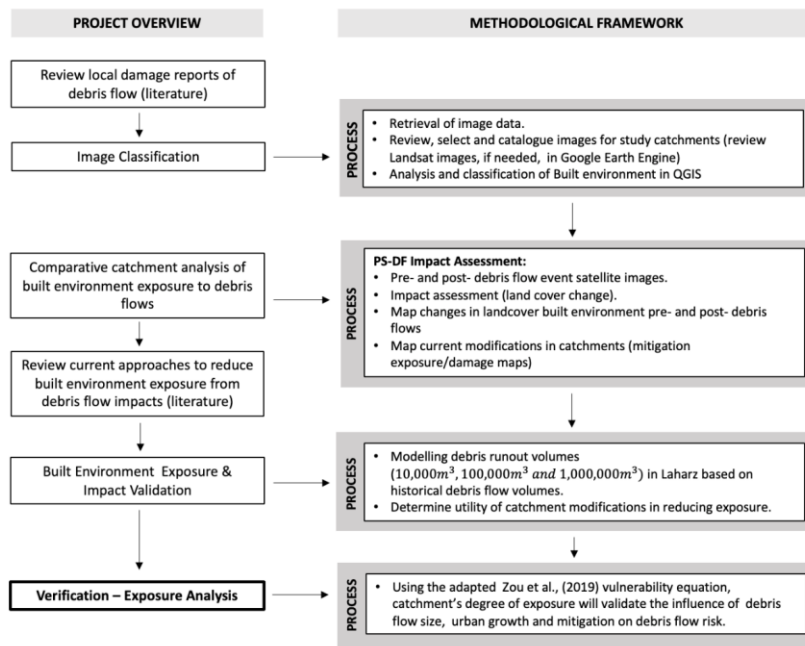


Figure 2: Schematic of our method. The key data sources comprise three multi-temporal datasets, including two from Fan et al. (2019a) covering debris flow and triggering rainfalls, as well as mitigation measures. The third dataset is adapted from Fan et al., (2019a) and highlights gully's with debris flow events post-2008 including information on the flow volume and presence of mitigation. Additional spatial data sources include aerial imagery from OpenStreetMap (OpenStreetMap contributors., 2023), World Settlement Footprint (World Settlement Footprint., 2019) and Shuttle Radar Topography Mission (SRTM) (Farr et al, 2007).

3.1 Data Classification

This study builds on existing multi-temporal debris flow datasets produced by Fan et al., (2019a). Dataset 1 has an aerial extent of 892 km^2 and presents the location and dimensions of debris flow events between 2008 and 2020. Dataset 2 presents a list of mitigative actions e.g., construction of check dams, taken between 2008–2011. We used an SRTM DEM to construct elevation profiles of Cutou, Chediguan and Xiaojia gullies to extract topographic characteristics to understand the mechanism of slope failure in the event of a rainfall-induced debris flow. These profiles facilitate morphological valley changes from debris flows to be identified. Through a comparative analysis of the 20th August 2019 debris flows in Cutou and Chediguan, we investigated the relative

174 difference in land use change in the two gullies from 2008 to 2019, with a focus on changes before and after the
175 2019 flow event.

176 Landscape modification from 2005 to 2019 were mapped using high resolution (0.5 to 2.5m) satellite images
177 (Table 1). We selected images with less than 50% cloud cover and cross-referenced the mapped features with
178 existing data sources in OpenStreetMap (OpenStreetMap contributors., 2023) and Dynamic World (Brown et al.,
179 2022). Where satellite imagery was unavailable, we used aerial photos obtained from Google Earth,
180 OpenStreetMap and World Settlement Footprint (World Settlement Footprint., 2019). It should be acknowledged
181 that platforms like OpenStreetMap offer a regional view of Wenchuan rather than a detailed local-scale with
182 mapping limited to main roads and 150 settlement polygons. However, this study's locations are unaffected by
183 this due to their position next to the G213 national highway and G4217 road.

184 **Table 1** Satellite and aerial imagery used for data analysis and interpretation of the built environment.
185
186

Data ID	Data Source	Acquisition Date	Resolution (m)
Aerial Satellite	Worldview (in QGIS – ‘Satellite’ XYZ tile)	2022	1.0
Satellite	Worldview (in Google Earth Pro., 2023)	10.12.2010 26.04.2011 03.04.2018 29.10.2019	1.0
Satellite	Planet	14.08.2019 24.08.2019	3.0
Satellite	Maxar Technologies (in Google Earth Pro., 2023)	09.09.2005 26.04.2011	3.0
Satellite	CNES/Airbus (in Google Earth Pro., 2023)	15.04.2015	1.0

187 We mapped features corresponding to human activities such as roads and properties. We highlighted at-risk zones
188 in Cutou, Chediguan, and Xiaojia. We focus on spotlighting areas of high debris flow exposure in Cutou and
189 Chediguan, comparing them with Xiaojia to evaluate the efficacy of check dams in mitigating potential debris
190 flow hazards downstream of the dams.
191
192

193 3.2 Modelling Future Debris Flow Runout and Building Exposure

194
195 Both Cutou and Chediguan had check dams installed after the 2008 earthquake, while the Xiaojia gully remained
196 unmodified. We compared the impacts of 2019 debris flows in Cutou and Chediguan gullies with a 2011 debris
197 flow event in the unmodified Xiaojia gully to identify the effectiveness of artificial dams in mitigating exposure
198 to post-seismic debris flows. By using scenario modelling we identified at which point, does the size of the hazard,
199 outweigh the mitigative capacity of the check dam to prevent overtopping. We mapped debris flows of differing
200 scales within each of our three catchments using LAHARZ. LAHARZ is a GIS toolkit for lahar hazard mapping
201 and modelling, developed by the USGS to calculate the area of inundation and cross sections based on empirical
202 scaling relationships between area and volume visualise debris flow paths based on an empirical set of equations
203 (Schilling., 2014; Iverson et al., 1998). These empirical relationships allow for the creation of realistic inundation
204 areas without a priori knowledge of the rheological parameters. The model simulates a debris flow triggered at a
205 source point located on a digital elevation model and with an initial source volume. The model calculates the flow
206 path downslope of the triggering location then generates a cross-section at each point downslope that represents
207 the depositional volume for that area (Iverson et al., 1998).
208 This toolkit was adopted due to its ability to accommodate varying flow volumes and provide details inundation
209 predictions. The model calculates runout extents using empirical equations that calculate the cross section of the
210 debris flow at every point along a flow path. LAHARZ makes three key assumptions: were made in our
211 adaptation of LAHARZ to model debris flow runout for this research. These are:
212 Steady-state flow, which conditions to simplify the complex hydrodynamics of debris flows.
213 Sediment storage effects modelled by reducing effective flow volumes upstream of check dam locations.
214 Depositional areas identified based on terrain slope thresholds, consistent with prior studies.

215 We implemented this model using the extension in ArcGIS (Schilling., 2014). We used the 30m resolution DEM
216 as an input, as it is the most reliable of the globally available DEMs. We identified the source areas of 2019 debris
217 flows for Chediguan and Cutou and the 2011 for Xiaojia (Cutou – 351603, 3473449; Chediguan – 350846,
218
219

Commented [IU2]: 1. Lines 143-226: The methodology section should include the rationale for the selection of model parameters and provide a sensitivity analysis to enhance the credibility of the model results. (R1C)

3. LAHARZ simulation, data processing, assumption, and technical details were missing. (R2C)

Formatted: No bullets or numbering

Formatted: No bullets or numbering

3453894; Xiaojia – 356666, 3439268) from satellite imagery and used these as the triggering locations for our simulations. We then prescribed three input volumes at each of these locations ($10^4 m^3$, $10^5 m^3$ and $10^6 m^3$). The flow volumes simulate a range of observed post-2008 debris flows, representing low, high, and extreme debris flows documented in the Fan et al., (2019a) datasets. The volumes we selected reflects the range of similar hazard events in comparable geomorphological settings such as other parts of China and Italy (Wu et al., 2016; Bernard et al., 2019). For catchments with check dams we added barriers at each check dam location by raising the cell count of the DEM by the height of the check dam obtained from field imagery.

that incorporate key factors such as LAHARZ requires three inputs, an initial material triggering volume, flow parameters (what are these) and a digital elevation model to derive the topography, slope, and mitigative structures like check dams (Iverson et al., 1998). This functionality enables simulation of future flow behaviours and aids in visualising potential debris flow impacts on the built environment and critical infrastructure. The model provides an estimate of flow extent from a given initial material volume, and can account for various factors such as topography, slope and mitigative structures which generates more detailed data outputs when simulating future flow behaviour. For each catchment we simulated three flow sizes that represent the range of observed post-2008 earthquake debris flow volumes: $10^4 m^3$, $10^5 m^3$ and $10^6 m^3$. These volumes represent low, high, and extreme debris flows derived from respectively based off of recorded post seismic debris flow occurrences post-2008 documented in the Fan et al., (2019a) datasets.

We note that there is currently a limited understanding of the maximum debris flow volumes in these catchments following the 2008 earthquake, the thresholds selected align with similar hazard events in comparable geomorphological settings in China, Italy and others, ensuring realistic scenario design and outcome predictions.

The simulations relied on using a 30m DEM for simulations due to data availability. We used the 30m resolution ASTER DEM as an input, as it is the most reliable. While a higher resolution 10m DEM would have likely improved predictive accuracy, particularly for extreme scenarios, the 30m DEM sufficiently captures topographic characteristics for scenario modelling of the selected catchments. Input data included: sediment volumes derived from a combination of previous field studies and historical records; We further defined channel dimensions measured estimated from optical satellite imagery (Worldview) evolution mapping, whereas; catchment delineation and flow path identification, conducted using ArcGIS tools to accurately represent sediment transport pathways; were defined in the model using standard ArcGIS algorithms. Flow parameters processed from were defined through a combination of literature, historical field data and remote sensing observations to refine inputs like channel slope and volume to runout relationships.

Three key assumptions were made in our adaptation of LAHARZ to model debris flow runout for this research. These are:

- Steady state flow conditions to simplify the complex hydrodynamics of debris flows.
- Sediment storage effects modelled by reducing effective flow volumes upstream of check dam locations.
- Depositional areas identified based on terrain slope thresholds, consistent with prior studies.

The mModel was validated calibration was achieved by comparing simulated runout extents with observed debris flows from post-2008 events. While a 30m resolution was the only available DEM for our study locations, we tested the sensitivity of DEM resolution on the extent of the final flow. A higher, 10m resolution DEM was available for the Cutou gully and we ran LAHARZ for that catchment. A sensitivity analysis was conducted to evaluate the impact of input parameter variability, including DEM resolution and flow volumes. While the a higher resolution 10m DEM created a more effective flow path compared to the mapped data, the flow depositional area was similar in both the 10m and 30m scenarios showed to improve depositional accuracy, particularly in extreme scenarios (RMSE 18m). Given the lack of a significant difference between the two DEM resolution we ran 30m scenarios across the three catchments. the 30m DEM adequately captures topographic characteristics for modelling scenarios in the selected catchments. Thad a reliable NSE score of 0.78 and RMSE of 25m for extreme flow volumes. We note that there is not a strong understanding currently of what controls the maximum size of debris flows within Wenchuan catchments, hence we cannot attribute a particular probability to each scenario.

In the analysis of post-seismic debris flow, vulnerability assessment plays a crucial role (Lo et al., 2012). However, adapting traditional vulnerability methods which analyse inherent fragility and the potential loss of elements at risk, both attainable through remote practises, calculating exposure with minimal onsite data, remains a challenge. We adapted a vulnerability model by Zou et al. (2019) to quantify the extent of exposure to the built environment at our three sites, Cutou, Chediguan and Xiaojia.

Formatted: Don't adjust space between Latin and Asian text, Don't adjust space between Asian text and numbers, Tab stops: 0.99 cm, Left + 1.98 cm, Left + 2.96 cm, Left + 3.95 cm, Left + 4.94 cm, Left + 5.93 cm, Left + 6.91 cm, Left + 7.9 cm, Left + 8.89 cm, Left + 9.88 cm, Left + 10.86 cm, Left + 11.85 cm, Left

Utilising satellite and/or aerial imagery and extracting spatial characteristics to identify both elements at risk as well as hazard-affected zones, our analysis facilitates the assessment of regional exposure without relying heavily on data collected onsite. Our model quantifies the susceptibility of the built environment to debris flow damage. The degree of exposure, E_{df} , is expressed as:

$$E_{df} = E_b \times C \pm M \quad (1)$$

E_b is the number of buildings damaged, and C is the fragility index of the elements at risk (Zou et al., 2019). Fragility values range from 0 to +1, with higher values indicating greater susceptibility to damage and/or failure. We assigned fragility values through using a mixture of literature and satellite images; buildings shown to be inundated or damaged in previous events or situated along the channel or gully mouth were given a value of 1, all other buildings were set a value of 0. These values were validated using historical damage reports, where available, from the 2008 earthquake recovery period to ensure applicability (Zeng et al., 2015; Wei et al., 2021; Petley et al., 2023). This approach allows for replicable application designs in similar hazard-prone areas.

The key difference between our method and that of Zou et al (2019) is the incorporation a modification factor, M , to account for the effectiveness of engineered measures like check dams in mitigating building damage and subsequent exposure. The mitigation factor, M , quantifies the influence of engineered measures, in this study check dams, on the vulnerability and subsequent exposure of buildings to debris flow impacts. The addition of this factor brings an evaluative element to the exposure assessment, quantifying the influence of check dams and assigning values ranging from -1.0 to +2.0 to reflect a spectrum of mitigation outcomes:

- $M = -1$: Effective mitigation of debris flows dynamics, resulting in a significant reduction in hazard exposure, as evidenced by a decrease in the number of buildings damaged during historical events following construction.
- $M = 0$: No mitigation present; exposure levels are entirely dependent on natural site conditions.
- $M = +1$: Ineffective mitigation; there is no reduction in the number of buildings impacted in recorded debris flow events following dam construction.
- $M = +2$: Mitigation increases exposure. Recorded events of similar volume show an increase in the number of buildings impacted following dam construction.

The above -1 to +2 scale was selected to capture a nuanced relationship between mitigation effectiveness and vulnerability. A reduction in M (e.g., -1) lowers hazard exposure by reducing flow impacts at critical locations, thereby decreasing E_{df} in the exposure equation. Conversely, an increase in M (e.g., +2) elevates exposure, as development in hazard-prone areas amplifies the potential for damage. For example, a decrease in M by one unit (from 0 to -1) reflects an improvement in flow attenuation due to effective check dams, reducing overall exposure. Conversely, an increase in M by one unit (from 0 to +1) signifies a scenario where mitigation fails, e.g. the 2019 debris flow event in Cutou, maintaining high exposure levels. At $M = +2$, exposure exceeds natural vulnerability due to increased hazard presence caused by intensified land use near mitigation structures.

This scale was developed through a combination of evaluating present hazard mitigation theory and analysing historical data, particularly from the 2008 earthquake. For instance, gullies will be assigned a value of '+1' if modifications prove unsuccessful, '0' if no modifications are present, or '-1' if protection is offered by the mitigation measures. This recovery. Moreover, this approach, based upon the methodology proposed by Zou et al. (2019), allows for an assessment of exposure by considering both the physical resistance of buildings and the efficacy of mitigation efforts.

4. Results

4.1 Assumptions

In constructing the building inventory for Cutou and Chediguan, a comprehensive approach was taken to ensure accuracy and completeness. We used aerial and satellite imagery spanning 14 years, with a focus on mapping changes from 2011 to 2019. This involved careful analysis to delineate individual buildings, considering variations in size, shape, and spatial arrangement. Mapping efforts for Xiaojia were limited to 2010-2011 due to suboptimal

Commented [IU3]: 1. Line 217 The facility value and related parameters selection were overlooked, and that increase the vagueness of application process in case the reader was interesting in similar application design. (R2C)

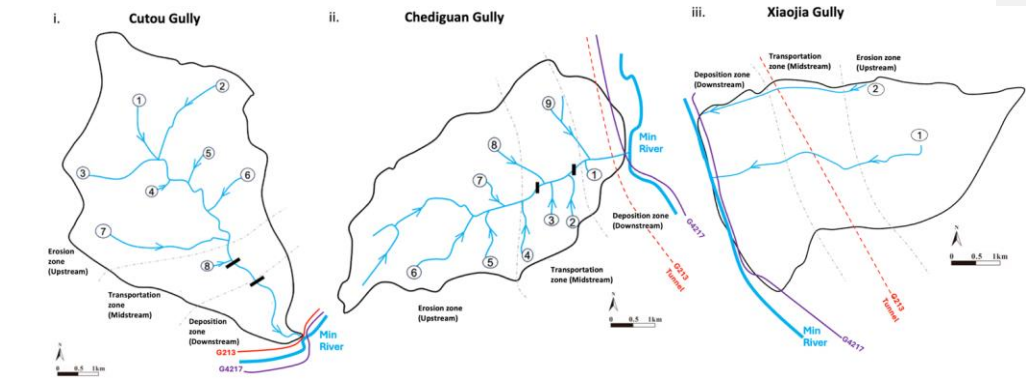
Commented [IU4]: 2. The justification of using -1 to +2 as units of measure to be inserted and its quantification relationship to vulnerability value is missing. (R2C)

339 image quality. Our approach incorporated assumptions regarding structural categorisation, including residential,
340 industrial, and commercial buildings. These assumptions were informed by existing literature on local building
341 typologies and architectural styles (Hao et al., 2013; Hao et al., 2012) and aerial photograph analysis from
342 platforms such as Google Earth and Dynamic World. By amalgamating diverse information sources, we aimed to
343 create a comprehensive inventory that correctly reflects the built environment of the study area.
344

345 Additionally, we used a 30-meter Digital Elevation Model (DEM) obtained from the SRTM dataset (Farr et al.,
346 2007). However, it is necessary to acknowledge the limitations of this data, particularly its ~~poor~~ low resolution
347 and subsequent blockiness, which potentially hindered detailed topographical analysis. Despite this, the DEM
348 provided valuable contextual information for understanding the terrain and its influence on building distribution
349 and spatial patterns within the three sites. Furthermore, while using the empirical LAHARZ model for debris flow
350 inundation mapping, we had to account for a degree of approximation in both aerial coverage and debris flow
351 inundation due to the 30m resolution of the DEM file.
352

353
354 **4.2 Mapping Post-Earthquake Risk**
355

356 Analysis of satellite imagery from 2005 to 2019, and topographic profiles, reveals channel widening, deepening,
357 aggradation, and deposition, likely attributed to the mobilisation of coseismic deposits and subsequent debris flow
358 occurrences (Zhang et al., 2015; Wang et al., 2018) (Fig 3). These observations allowed us to determine the zones
359 of erosion, transportation, and deposition for each gully and to track changes over time. Hydrological and
360 geomorphological analysis examines landscape morphology to identify erosional and depositional features i.e.,
361 scarring, changes to river channel, sediment buildup (Fig 4). By integrating the above, we delineated erosion-
362 prone areas, which permitted sediment transport routes to be approximated, and identify locations of sediment
363 deposition along the hydrological profile.



364 **Figure 3:** Hydrological profiles for the 3 study sites. Dam locations approximated for Cutou (i) and Chediguan
365 (ii) based on a combination satellite imagery. Streams and main tributaries are numbered. Catchment profiles have
366 been segmented into 3 zones – ‘erosion’, ‘transportation’ and ‘deposition’ and key infrastructure annotated.
367

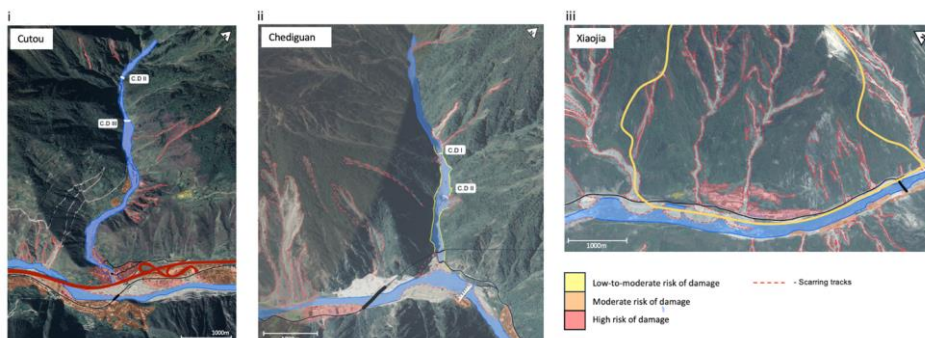


Figure 4: Satellite images of the 3 study locations highlighting areas of scarring from previous debris flow activity and areas of increased erosion (© Google Earth 2019). Dam locations have been approximated for Cutou (i) and Chediguan (ii). The built environment has been shaded based upon risk of damage based upon proximity to areas of high erosion. Critical infrastructure has been added where appropriate: black line represents the G4217 road with the thicker sections representing bridges and the dashed lines, tunnels. The red line in (i) is the G213 Highway.

In Cutou and Chediguan, deposition patterns shifted post-earthquake, particularly following the construction of check dams. Increased deposition occurs behind check dams compared to meander bends and basal slopes of the debris fan, demonstrating the effective sediment trapping of the check dams (Wang et al., 2019). Regarding the erosion patterns in Xiaojia, we observed common patterns in the upper gully sections at higher elevations, with deposition occurring at the basal slopes. This is due to the absence of structural alterations to the channel, permitting sediment to be transported to the channel and subsequent river outlet directly. The deposition patterns in Cutou and Chediguan, are strongly controlled by the distribution of check dams, in the middle and downstream portions of the catchment (Wang et al., 2019). The complex interplay between natural and anthropogenic factors demonstrates the dynamic evolution of risk in post-earthquake catchments and highlights the role of check dams in both mitigating and potentially exacerbating risk.

The landscape morphology prior to the 2008 earthquake was marked by extensive vegetation (over 70% of land cover) and minimal permanent engineered features. Cutou gully contained a widespread distribution of buildings along both the mid and lower slopes. Figure 5 shows the growth of the built environment between 2005 and 2019 in Cutou and Chediguan and between 2010 to 2011 in Xiaojia. The built environment in Cutou is concentrated within the transportation and deposition zones on both sides on the stream. In Chediguan by comparison we observed fewer residential structures, mostly industry and some commercial structures. Additionally, buildings in the gully are more spread out than in Cutou highlighted by the isolated settlements to the south of the catchment and single industrial site situated in the basin. Post-2008, noticeable tracks of scarring from debris flows are concentrated downstream of dams 2 and 3 in Cutou (Fig 4(i)), and upstream of dams 1 and 2 in Chediguan (Fig 4(ii)). Deposition patterns are evident downstream of all modifications, forming a depositional zone, encompassing approximately 15% and 20% of the built environment in 2019 within the transportation zone of Cutou and Chediguan, respectively.

Importantly, Xiaojia was chosen as the comparative catchment due to the absence of engineered mitigation such as check dams. This analysis of Xiaojia therefore offers a critical perspective enables comparisons on the effectiveness and limitations of engineering approaches applied to Cutou and Chediguan. In contrast, Xiaojia, the lack of lacking engineered dam structures, results in different erosion and deposition dynamics patterns compared to the other two catchments. Distinct patterns of upstream erosion upstream and downstream deposition are observed, contrasting with the more controlled downstream environments in the modified gullies, where. Notably, between check dam structures in Cutou and Chediguan, deposition occurs on the northern channel flank and pronounced erosion on the southern flank. The data availability for building types, quality and spatial distribution was limited to remote sensing images and few literature sources, which restricts our ability to thoroughly assess how specific building characteristics, such as materials, influence the exposure of the built environment to debris flow risk hazard. This is particularly evident in Xiaojia, where more specific input data would be beneficial for understanding the role of urbanisation and construction practices on risk levels.

Commented [IU5]: 1. Expand the analysis of the Xiaojia area to explore the specific reasons for its low exposure changes, such as natural terrain barriers, land-use planning, or building quality.
(R1C)

Our analysis of Xiaojia unveils no discernible relationship between building development and heightened exposure, particularly to residential and critical infrastructure. This lack of correlation is potentially linked to factors beyond simple urbanisation patterns, like construction quality, building regulations, presence of natural barriers, and effectiveness of mitigation measures. Natural terrain barriers observed in this gully including steep slopes and rocky outcrops, could limit the extent of debris flow impacts by reducing the mobility of debris and offering natural protection to certain areas. To fully understand this observation, further investigation into the above variables is warranted. The absence of significant urban expansion, particularly post-earthquake in Xiaojia may be a key factor in mitigating exposure. This area has experienced less intensive development compared to Cutou and Chediguan, where urban expansion following the implementation of check dams potentially increased exposure to debris flow hazards. Furthermore, the building quality in Xiaojia may play a significant role in influencing its overall vulnerability. Without more detailed building-specific data, it is possible that buildings in Xiaojia may be of higher structural integrity or designed to withstand environmental stressors better than those in more developed catchments.

Additionally, detailed mapping of past debris flow events and their impacts on the built environment could provide insights into the specific mechanisms influencing vulnerability in Xiaojia. By conducting a more comprehensive analysis that considers these factors – especially in terms of land-use planning, construction standards and the role of natural terrain features at the local scale, we can gain a better understanding of the complex interactions between building development and exposure to natural hazards in Xiaojia. This, in turn, can inform more effective risk management and mitigation strategies tailored to the unique characteristics of the area. Development in Xiaojia primarily concentrates on the lower slopes (Fig 5(i) and (ii)) at the gully mouth, featuring the construction of major roads and highways (G213 and G2417), alongside the expansion of existing residential areas. Chediguan exhibits a less marked land cover transformation, owing to roads being directed through mountain tunnels. Notably, development in Xiaojia mainly surges post-earthquake up to 2010, with only minor construction activities documented thereafter (Fig 5(iii)).

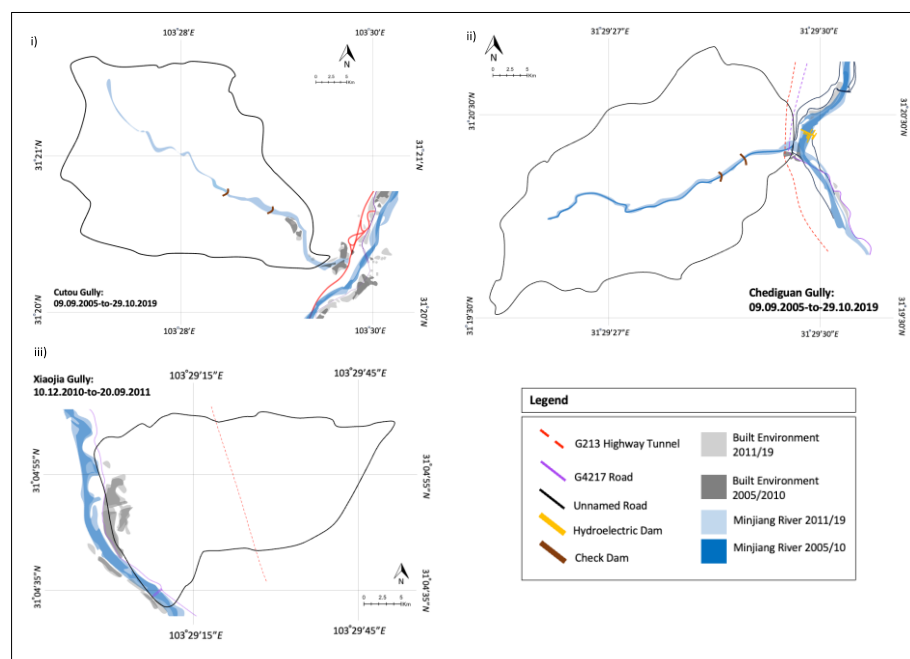


Figure 5: Evolution of the built environment and key infrastructure in (i) Cutou, (ii) Chediguan and (iii) Xiaojia post-earthquake between 2005 and 2019.

We mapped the number of buildings impacted by debris flows that occurred within the Chediguan and Cutou gullies. At 02:00 a large-scale debris flows hit Chediguan, impacting numerous structures, at around 05:00 a similar debris flow hit Cutou with significant inundation noted. 79 of the 197 buildings (40%) in Cutou (Fig 5(i)) were impacted by the flow i.e., flooded, damaged, or destroyed. Buildings in Chediguan were less impacted by that event with 7 out of the total 69 (10.1%). We combined the satellite imagery with the datasets produced by Wang (2022) which supported our observations of check dam overtopping in both Cutou and Chediguan during the 2019 event. In 2011 a similar event in Xiaojia impacted approximately 5 of the 43 (11.6%) buildings in the gully (Fig 5(iii)).

4.3 Modelling exposure to post-earthquake debris flows

Our LAHARZ simulations demonstrate a clear correlation between exposure and debris flow runout, revealing a notable increase in building damage as runout volumes escalate from low ($10,000\text{m}^3$) to high ($100,000\text{m}^3$) and extreme ($1,000,000\text{m}^3$) scenarios across all catchments. Despite the presence of check dams, the 2019 debris flows recorded runout volumes significantly larger than the maximum simulated volume, resulting in substantial building and infrastructural loss in Cutou (Fig 6(i)) and Chediguan (Fig 6(ii)).

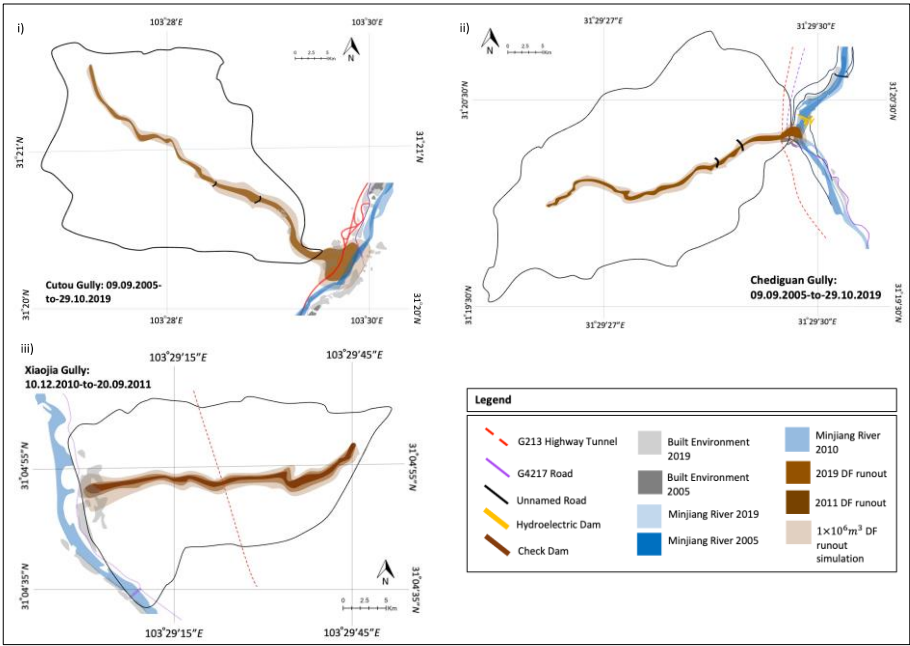


Figure 6: Debris flow runouts for 2019 in Cutou (i) and Chediguan(ii) and 2011 in Xiaojia (iii) underlain by the extreme LAHARZ runout scenario. Low and high runouts are not displayed as they are not easy to visualise at map scale.

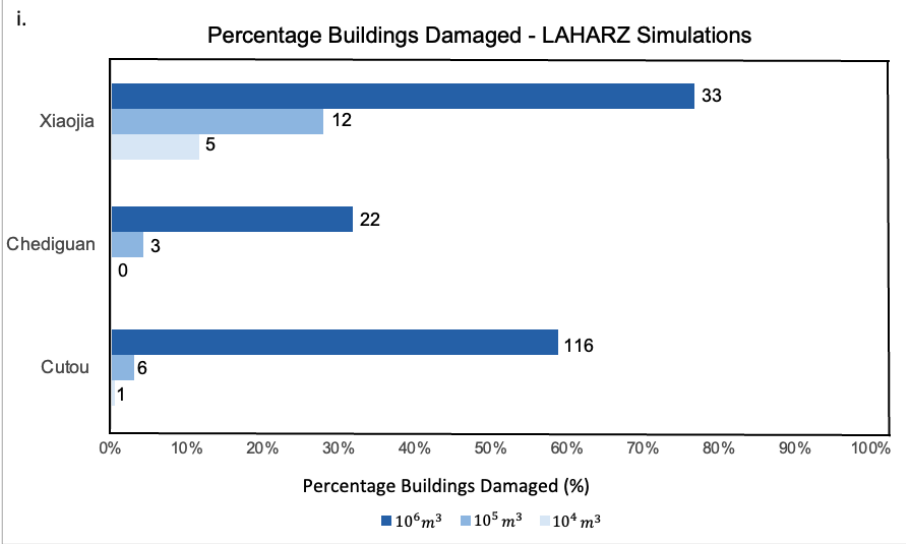
We examined the temporal dynamics of building changes within the three gullies in response to check dam development, while also considering the implications of the levee effect (fig 6). Our simulations revealed the effectiveness of engineered measures in mitigating exposure to debris flow events. In both Cutou and Chediguan, the presence of check dams led to reduced exposure at low and high debris flow volumes (fig 7(i) and (ii)). However, the mitigative structure provides no discernible protection against extreme debris flows. Notably, Cutou consistently exhibited elevated exposure to debris flow runout compared to Chediguan. The unengineered Xiaojia provided an informative comparison (fig 6(iii)), highlighting the effectiveness of check dams at low and high debris flow volumes. Xiaojia's post-2011 expansion appeared restrained, indicating a potential adaptive response

475 following debris flow events. In contrast, substantial expansion occurred in Cutou and Chediguan between 2011
476 and 2019, despite experiencing a debris flow event in 2013, suggesting the impact of check dams implemented
477 post-2013.

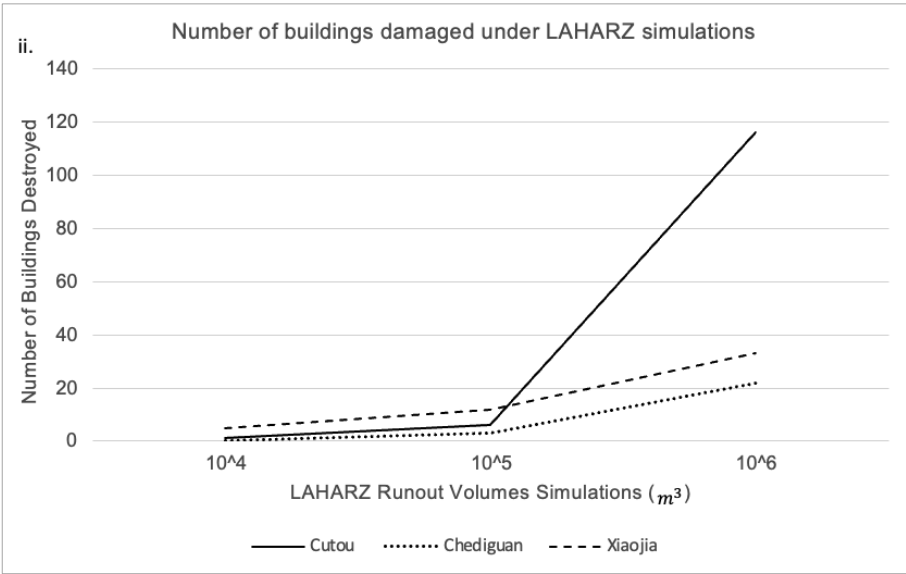
478
479 Furthermore, the incremental increase between high and extreme simulations in Xiaojia paralleled Chediguan's
480 gradual incline, diverging from Cutou's steep escalation. Xiaojia sustained a maximum building damage of 33%
481 under extreme scenarios, compared with 59% in Cutou and 22% in Chediguan. This discrepancy suggests that the
482 optimal efficiency of check dams may be surpassed, urging consideration of additional factors such as the
483 landscape's inherent resilience. Our observations underscore the nuanced variability in the effectiveness of check
484 dams, influenced by contextual factors and landscape characteristics.

485
486
487
488
489
490
491
492
493
494
495
496
497
498
499
500
501
502
503
504
505
506
507
508
509
510

§11



Commented [IU6]: 4. Fig. 7 and the amount of buildings, types, and degree of vulnerability in terms of economic or physical were missing. (R2C)



§12
§13
§14
§15
§16
§17
§18
§19
§20

Figure 7: Built environment impacts from three debris flow scenarios modelled using LAHARZ at Cutou, Chediguan and Xiaojia. (i). Percentage of buildings damaged as a proportion of total buildings (Cutou – 197, Chediguan – 69 and Xiaojia – 43) in each scenario. The numbers at the end of the bars are the number of buildings damaged buildings in that debris flow scenario. (ii) Total number of buildings damaged by each simulated debris flow.

Figure 7 illustrates how a tenfold increase in runoff volume corresponds to building damage, with a discernible rise in impacted building numbers noted between low and high scenarios, and a significant incline between high and extreme scenarios across all catchments. These simulations provide valuable insights into the efficacy of engineered mitigation structures. While check dams in Cutou and Chediguan effectively reduce exposure at low and high runoff volumes, concerns arise when surpassing the maximum capacity. Urbanization emerges as a significant contributing factor impacting exposure and future risk, with the presence of check dams during the 2019 events significantly contributing to the built environment's exposure. However, due to the lack of available data on building materials in these three regions, we were unable to quantify their influence on structural vulnerability. As a result, exposure was determined to be the primary contributing factor to building damage. To fully understand the effect of check dams and validate our statistical approach, comprehensive numerical analysis of multiple hazard events in each gully is necessary. This sub-section addresses the elements driving hazard-related risk scenarios, including the trigger event, return period, and level of damage, and underscores the importance of considering these factors when suggesting and implementing modifications.

The exposure model is applied to historical events (2019 and 2011) and LAHARZ simulations, showcasing changes in the degree of exposure across the catchments with increasing debris flow runoff volumes (Fig 8). Consistent with earlier observations in exposure, Cutou exhibits a heightened vulnerability to debris flows at 64% after the 2019 event, followed by Chediguan at 52% and Xiaojia with 2% in 2011. A discernible change in building exposure is observed between the high and extreme scenarios across all catchments. The most influential factor in overall vulnerability remains the number of buildings, highlighting urbanization as a contributing factor impacting both exposure and physical vulnerability. Moreover, the presence of failed check dams in Cutou and Chediguan during the 2019 events significantly contributes to their physical vulnerability.

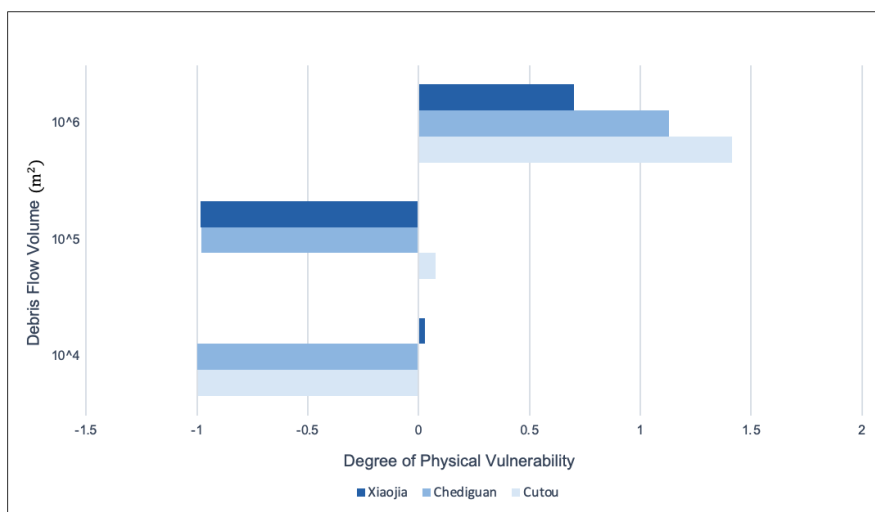


Figure 8: Changes in the degree of exposure with increasing runoff volumes using the exposure model developed in equation 1. The 2011 and 2019 debris flows are also noted as a base marker from an observed hazard event.

5. Discussion

Post-earthquake structural interventions influence the volume and spatial distribution of sediment within the catchment. Our observations show that check dams act as local depocentres within the catchment, often storing large volumes of sediment upstream of the majority of building development. The choices made about post-earthquake development of the built environment, particularly housing, and mitigative measures like check dams, evolve rapidly without a clear approach to mitigating adverse long-term consequences of sediment retention behind dams (McGuire et al., 2017). Additionally, the processes driving geological disasters in the complex landscape of the Longmenshan occur at different timescales to the rapid socio-economic development in the region (Chen et al., 2022).

Commented [IU7]: 4. Fig. 7 and the amount of buildings, types, and degree of vulnerability in terms of economic or physical were missing. (R2C)

Although our analysis focuses on smaller-scale communities, the implications drawn from our findings echo those of broader studies. For instance, Arrogante-Funes et al. (2021)'s extensive investigation into hazard mitigation strategies in larger geographical regions, drew parallels to the effectiveness and limitations of mitigation measures to debris flows. Similarly, Chen et al. (2021) provided insights into the complexities of hazard mitigation, emphasising the necessity of adaptive responses considering local contexts. This aligns with our analysis that each gully must be assessed and mitigated individually rather than collectively to account for local geological and hydrological influences on mitigation effectiveness. Moreover, Li et al. (2018) examined the long-term impact of engineering interventions, noting the variability in check dams effectiveness over time. This supports our conclusion that the diminishing effectiveness of check dams is likely the result of sediment accumulation and structural degradation and highlights the necessity for their continued maintenance post-construction in addition to adaptive mitigation strategies. Furthermore, Eidsvig et al. (2014) and Tang et al. (2011) explored the interplay between socio-economic factors and hazard vulnerability, emphasising that community resilience is directly linked to economic resource availability and social cohesion. This corroborates our understanding that debris flow mitigation is a multifaceted issue, and socio-economic conditions are integral to their success. By situating our findings within the broader context delineated by these studies, we accentuate the relevance and applicability of our research beyond the confines of the specific communities under study.

Open check dams, similar to those established in Cutou and Chediguan, play a pivotal role in bed stabilization, slope reduction, and the regulation of sediment transport (Bernard et al., 2019). However, inadequate understanding of post-earthquake debris flow characteristics has led to the failure of many newly constructed engineered structures to mitigate hazards effectively, amplifying damage instead (Chang et al., 2022). During the August 2019 debris flow, Cutou experienced the highest inundation, with 40% of surveyed structures directly affected, including critical infrastructure like the G4217 highway bridge. In Chediguan, despite a declined industrial presence, debris flow impacts affected 7% of structures. The presence of check dams in both locations contributed to raised exposure and hazard impacts during the 2019 event, with overtopping and damage to dam sections recorded.

We conducted LAHARZ scenarios to predict potential exposure to debris flows with volumes that have been observed within the catchments and the region. Our results highlighted a clear correlation between exposure and debris flow runoff, showing notable increases in building damage as runoff volumes escalated from low to extreme across all catchments. We observed two key elements to the role of check dams in affecting exposure to debris flows. When empty, check dams are effective at mitigating the effects of small and medium volume debris flows. Yet, they are not effective at mitigating the largest of debris flows observed in this region. Large runoff volumes in the 2019 debris flows resulted in substantial building and infrastructural loss in both Cutou and Chediguan, suggesting a negative contribution from damaged check dams. Cutou was found to be highly exposed to extreme debris flow volumes, a result of its raised development level situated at the basal slopes. The fact that Xiaojia was found to possess the least exposure to the most extreme debris flow volume suggests that there may be an adaptive component to debris flow mitigation in catchments without significant check dam development. These findings suggest that urban development and debris flow risk co-evolve based on the nature of the structural interventions the studied areas.

Our analysis of erosion, transportation, and deposition zones for each gully revealed significant changes in landscape morphology post-earthquake, likely attributed to mobilised coseismic deposits and subsequent debris flow occurrences. The presence of check dams influenced deposition patterns, with mid-to-downstream trends indicating effective sediment retention in Cutou and Chediguan, while Xiaojia exhibited typical erosion-deposition behaviour. Our findings can be supported by a similar occurrence during the "8.13" debris flow event in Wenjiagou. The damage and subsequent failure of mitigative check dams led to the inundation of 490 houses or more recently, a debris flow in the Miansi and Weizhou townships on 27 June 2023 blocked the valley in the first instance before breaching the dam and causing 7 fatalities (Petley., 2023). Further research is thus imperative to devise appropriate mitigation approaches for post-seismic debris flows. Whilst existing literature has underscored the physical effectiveness of check dams in reducing exposure to debris flow impacts within Alpine terrains (Piton et al., 2016), it should be noted that their primary function extends beyond this to also provide socio- economic and political reassurance (Wu et al., 2012; Chen et al., 2022)

The findings of our paper support the theory of the levee effect by demonstrating how the implementation of mitigative measures, such as check dams, can inadvertently increase exposure levels and risk perception in hazard-prone areas. The interplay between engineering solutions and the built environment as highlighted in our study through analysis of the 2011 and 2019 events as well as the LAHARZ simulations, illustrates the levee effect. Similar to previous studies on flooding and the levee effect, [Similar to previous studies on flooding, for example](#)

(e.g. Collenteur et al., (2015), our paper suggests that the perceived reduction in hazard risk due to mitigative structures can lead to increased levels of exposure due to raised development in debris flow-prone regions. This effect is particularly evident in the Cutou catchment where urban expansion occurred post-dam construction, despite the region's repeated occurrence of continuous vulnerability to high magnitude debris flows. This suggests a -This phenomenon reflects the distorted perception of hazard risk, which ultimately drives urbanisation into vulnerable areas (Chen et al., 2015; Ao et al., 2020).

The levee effect can influence exposure to large-scale debris flow events by inadvertently increasing risk in areas protected by engineered mitigation structures, such as check dams. This occurs because the perceived safety provided by these structures can encourage development in vulnerable areas, which might otherwise remain uninhabited due to their high-risk nature. This phenomenon is best evidenced in our paper by the Cutou catchment, where the construction of check dams in 2013 coincided with widespread urban expansion, despite ongoing small-scale debris flow activity in the area. Subsequently, building exposure increased by 64% post-2008, underscoring the risk amplification associated with structural mitigation. This observation highlights the necessity of coupling structural interventions with strategies that address residual risks and foster community awareness of long-term hazard vulnerabilities. The 2019 debris flow event exemplified the risks associated with this effect, as the flow overtopped the check dams and used the stored material as a secondary fuel, significantly amplifying the impact. As a result, 40% of surveyed buildings were inundated, demonstrating how the levee effect can potentially escalate exposure to large-scale debris flow events.

Our LAHARZ simulations further reinforce the limitations of engineered structures as the sole mitigative measure in alpine environments; urbanisation of mountainous terrains further complicates the balance between technological advancements and geological hazards (Zhang, S et al., 2014; Zhang and Li., 2020; Luo et al., 2023). Despite the presence of check dams, our extreme runoff volume resulted in significant impacts on the built environment in Cutou and Chediguan, including overtopping and dam failure. The use of these simulations emphasises the challenges of reducing exposure to at-risk structures and highlights the unpredictable nature of debris flow occurrences. Moreover, our findings relating to the altered patterns of erosion and deposition emphasise the relationship between natural topography, engineered interventions, and risk perception in post-seismic debris flows. Urbanisation exacerbates this complexity, influencing exposure and physical vulnerability through deposit remobilisation. Our LAHARZ simulations serve as a practical demonstration of the levee effect, illustrating how engineered structures may not provide adequate protection against runoff volumes similar to the extreme simulation, thereby reinforcing the importance of considering the levee effect in debris flow risk management. The unpredictable nature of debris flow occurrences from pinpointing their location and timing to ascertaining their volume and velocity ultimately means that the concept of the 'levee effect' remains core to the issue of debris flows in post-seismic Sichuan (Cucchiaro et al., 2019a; Tang et al., 2022).

Whilst our findings are not able to definitively determine conclusively the prevalence of the levee effect with regards to development in post-seismic environments like Sichuan, we are able to hypothesise that the implementation of mitigative structures like check dams may this theory. From our study, we are able to posit that the implementation of mitigative check dams may inadvertently increase exposure levels to large-scale debris flow events by creating a false sense of safety. Although While our investigation does not fully explore this phenomenon, our outcomes suggest that the development of infrastructure in areas perceived to be safe due to the presence of engineered structures may amplify risk hazard exposure. This our outcomes highlights the limitations of solely relying on engineered interventions in reducing exposure to at-risk structures under the extreme LAHARZ scenario. Furthermore, we highlighted the complex interplay between engineering solutions and human behaviour, warranting further investigation (Papathoma-Köhle et al., 2011; Gong et al., 2021). By emphasising the challenges and limitations of engineered structures in mitigating debris flow impacts, we underscore the need for comprehensive risk management strategies that consider the complexities of urbanization and flow-based hazards in mountainous terrains.

Despite the presence of these engineered interventions, our analysis demonstrates significant exposure levels and infrastructure damage during extreme debris flow events. This discrepancy between perceived risk reduction and actual hazard exposure underscores the need for a more comprehensive understanding of risk perception in the context of hazard mitigation strategies. Moreover, our study highlights the importance of considering human behaviour and decision-making processes in the design and implementation of risk management measures. Future research should focus on elucidating the mechanisms driving risk perception in hazard-prone areas and developing strategies to bridge the gap between perceived and actual risk to enhance the effectiveness of mitigation efforts.

6. Conclusion

Commented [IU8]: 1. Could authors further explain how the 'levee effect' influence exposure of large-scale debris flow events?
(RIC)

Our study investigated the ~~changing exposure to debris flows in Cutou~~ ~~impact of debris flows in Cutou~~. Chediguan and Xiaojia since the 2008 Wenchuan earthquake. We used high resolution satellite imagery to build a time series of building inventories between 2005 and 2019. Despite recurrent debris flow occurrences between 2010 to 2013, ~~we observed increased urban developments across all three gullies to varying extents until 2015.~~ ~~we found increased urban development across all three gullies until 2015.~~

We ~~identified found~~ significant differences ~~in the impacts of between the~~ debris flow events ~~in 2011 and 2019 respectively.~~ ~~of 2019 and 2011.~~ In the August 2019 debris flow, Cutou experienced the highest inundation, with 40% of surveyed structures directly affected, including critical infrastructure such as the G4217 highway bridge. In contrast, the 2011 event in Xiaojia impacted approximately 11.6% of buildings in the gully, indicating a lower level of damage compared to Cutou. The presence of check dams in Cutou and Chediguan contributed to ~~increased~~ ~~raised~~ exposure and hazard impacts during the 2019 event, with overtopping and damage to dam sections recorded at both locations. However, despite the presence of these mitigative structures, the impact on the built environment was significant, suggesting limitations in their effectiveness, particularly during extreme runoff volumes. Our Laharz simulations demonstrated a clear correlation between exposure and debris flow runoff, revealing a notable increase in building damage as runoff volumes increased from low to high and finally extreme scenarios across all catchments. Despite the presence of check dams, the simulations indicated that these structures were unable to reduce the impacts on the built environment, especially during extreme events. ~~Furthermore~~ ~~Moreover~~, our analysis ~~highlighted a heightened level of~~ ~~of building damage and exposure patterns highlighted a heightened level of~~ built environment exposure in Cutou ~~to debris flows~~ compared to Chediguan and Xiaojia ~~driven by.~~ ~~This susceptibility was attributed to factors such as the~~ urbanisation, the presence of critical infrastructure, and the effectiveness of mitigative measures.

Our findings suggest that the presence and location of check dam in gully channels ~~likely increased building exposure and contributed to probably facilitated in increasing building exposure and at the~~ levee effect. ~~This raises concerns about the long-term implications, including~~ ~~in addition to raising concerns about their long-term implications i.e.,~~ structural integrity, maintenance and clearing. LAHARZ modelling provides comprehension of check dam efficacy, raising concerns for Cutou and Chediguan in high-to-extreme runoff events. Further, the combined use of the LAHARZ GIS toolkit and exposure analysis contributes to a holistic understanding of the risk landscape, informing strategies for enhanced disaster resilience and sustainable development in vulnerable areas.

The assumptions and subsequent considerations highlighted ~~throughout our study underscore the complexities of underpin our methodological approach in understanding~~ how the presence of check dams, as a mitigative structure, influences land-use planning and development in hazard-prone areas. ~~The~~ ~~se factors~~ ensure that the data outputs are comprehensive but also reflective of the inherent complexities of the study area and limitations in available data sources and analytical tools. We ~~have~~ highlighted a relationship between the presence of engineered measures like check dams alongside the built environment, ~~showing how this relationship has contributed to increased debris flow impacts post-2008 earthquake in Sichuan, particularly with increased debris flow impacts post-2008 earthquake in Sichuan~~ provinces along the Minjiang. Our results emphasise the need for a multi-faceted approach ~~to risk management,~~ integrating socio-economic development ~~and addressing the in debris flow prone regions,~~ ~~considering the~~ paradoxical role of mitigative structures ~~in shaping on~~ public perception to hazard exposure and vulnerability. Understanding these complexities is vital for informed decision-making and effective debris flow risk management.

Overall, our findings have indicated that the 2019 debris flow events ~~caused~~ ~~resulted in~~ more significant damage and higher exposure levels compared to the 2011 flow, emphasising the need for comprehensive risk management strategies in debris flow-prone areas.

Acknowledgements

EH is supported by the BGS-NERC National Capability grant 'Geosciences to tackle Global Environmental Challenges' (NERC reference NE/X006255/1) and publishes with permission from the Executive Director of the British Geological Survey.

References

Ao, Y., Huang, K., Wang, Y., Wang, Q. and Martek, I. 2020. Influence of built environment and risk perception on seismic evacuation behavior: Evidence from rural areas affected by Wenchuan earthquake. International journal of disaster risk reduction: IJDRR 46(101504), p. 101504. Available at: <https://www.sciencedirect.com/science/article/pii/S2212420919313500>.

Commented [IU9]: 4. The introduction and conclusion sections should better align with the research objectives. (R1C)

- Arrogante-Funes, P., Bruzón, A.G., Arrogante-Funes, F., Ramos-Bernal, R.N. and Vázquez-Jiménez, R. 2021. Integration of vulnerability and hazard factors for landslide risk assessment. *International journal of environmental research and public health* 18(22), p. 11987. Available at: <http://dx.doi.org/10.3390/ijerph182211987>.
- Bernard, M., Boreggio, M., Degetto, M. and Gregoretti, C. 2019. Model-based approach for design and performance evaluation of works controlling stony debris flows with an application to a case study at Rovina di Cancia (Venetian Dolomites, Northeast Italy). *The Science of the total environment* 688, pp. 1373–1388. Available at: <https://www.sciencedirect.com/science/article/pii/S0048969719325288>.
- Brown, C. F. *et al.* Dynamic world, near real-time global 10 m land use land cover mapping. *Scientific Data* 9, 251 (2022).
- Chang, M., Luo, C., Wu, B. and Xiang, L. 2022. Catastrophe process of outburst debris flow triggered by the landslide dam failure. *Journal of hydrology* 609(127729), p. 127729. Available at: <https://www.sciencedirect.com/science/article/pii/S0022169422003043>.
- Chen, N.-S., Hu, G.-S., Deng, M.-F., Zhou, W., Yang, C.-L., Han, D. and Deng, J.-H. 2011. Impact of earthquake on debris flows — a case study on the Wenchuan earthquake. *Journal of earthquake and tsunami* 05(05), pp. 493–508. Available at: <http://dx.doi.org/10.1142/s1793431111001212>.
- Chen, X., Cui, P., You, Y., Chen, J. and Li, D. 2015. Engineering measures for debris flow hazard mitigation in the Wenchuan earthquake area. *Engineering geology* 194, pp. 73–85. Available at: <https://www.sciencedirect.com/science/article/pii/S0013795214002579>.
- Chen, M. *et al.* 2021. Quantitative assessment of physical fragility of buildings to the debris flow on 20 August 2019 in the Cutou gully, Wenchuan, southwestern China. *Engineering geology* 293(106319), p. 106319. Available at: <https://www.sciencedirect.com/science/article/pii/S0013795221003306>.
- Chen, Y., Song, J., Zhong, S., Liu, Z. and Gao, W. 2022. Effect of destructive earthquake on the population-economy-space urbanization at county level-a case study on Dujiangyan county, China. *Sustainable cities and society* 76(103345), p. 103345. Available at: <http://dx.doi.org/10.1016/j.scs.2021.103345>.
- Collenteur, R. A., de Moel, H., Jongman, B., & Di Baldassarre, G. (2015). The failed-levee effect: Do societies learn from flood disasters? *Natural Hazards (Dordrecht, Netherlands)*, 76(1), 373–388. <https://doi.org/10.1007/s11069-014-1496-6>
- Costa, J.E. 1984. Physical geomorphology of debris flows. In: *Developments and Applications of Geomorphology*. Berlin, Heidelberg: Springer Berlin Heidelberg, pp. 268–269. Available at: http://dx.doi.org/10.1007/978-3-642-69759-3_9.
- Couvert, B., Lefebvre, B., Lefort, P., & Morin, E. (1991). Etude générale sur les seuils de correction torrentielle et les plages de dépôts. *Houille Blanche*, 77(6), 449–456. <https://doi.org/10.1051/lhb/1991043>
- Cruden, D.M. and Varnes, D.J. 1996. Landslides: Investigation and Mitigation. Chapter 3—Landslide Types and Processes. Transportation research board special report, 247. In: *Transportation research board special report* (247).
- Cucchiario, S. *et al.* 2019a. Geomorphic effectiveness of check dams in a debris-flow catchment using multi-temporal topographic surveys. *Catena* 174, pp. 73–83. Available at: <https://www.sciencedirect.com/science/article/pii/S0341816218304910>.
- Cucchiario, S., Cazorzi, F., Marchi, L., Crema, S., Beinat, A. and Cavalli, M. 2019b. Multi-temporal analysis of the role of check dams in a debris-flow channel: Linking structural and functional connectivity. *Geomorphology (Amsterdam, Netherlands)* 345(106844), p. 106844. Available at: <https://www.sciencedirect.com/science/article/pii/S0169555X1930323X>.
- Cui, P., Wei, F. Q., He, S. M., You, Y., Chen, X. Q., Li, Z. L., *et al.* (2008). Mountain Disasters Induced by the Earthquake of May 12 in Wenchuan and the Disasters Mitigation. *J. Mountain Sci.* 26 (3), 280–282. doi:10.35123/geo-expo_2017_4

797
798 Dai, Z., Huang, Y., Cheng, H. and Xu, Q. 2017. SPH model for fluid–structure interaction and its application to
799 debris flow impact estimation. *Landslides* 14(3), pp. 917–928. Available at: [http://dx.doi.org/10.1007/s10346-](http://dx.doi.org/10.1007/s10346-016-0777-4)
800 [016-0777-4](http://dx.doi.org/10.1007/s10346-016-0777-4).
801
802 Eidsvig, U.M.K., Papathoma-Köhle, M., Du, J., Glade, T. and Vangelsten, B.V. 2014. Quantification of model
803 uncertainty in debris flow vulnerability assessment. *Engineering geology* 181, pp. 15–26. Available at:
804 <https://www.sciencedirect.com/science/article/pii/S0013795214002051>.
805
806 Fan, X. et al. 2018. What we have learned from the 2008 Wenchuan Earthquake and its aftermath. A decade of
807 research and challenges. *Engineering geology* 241, pp. 25–32. Available at:
808 <https://www.sciencedirect.com/science/article/pii/S0013795218307233>.
809
810 Fan, X., Scaringi, G., Domènech, G., Yang, F., Guo, X., Dai, L., He, C., Xu, Q., and Huang, R. 2019a. Two
811 multi-temporal datasets that track the enhanced landsliding after the 2008 Wenchuan earthquake, *Earth Syst.*
812 *Sci. Data*, 11, 35–55, <https://doi.org/10.5194/essd-11-35-2019>
813
814 Fan, X., Scaringi, G., Korup, O., West, A. J., van Westen, C. J., Tanyas, H., Niels Hovius , Tristram C. Hales ,
815 Randall W. Jibson , Kate E. Allstadt , Limin Zhang , Stephen G. Evans , Chong Xu10, Gen Li4 , Xiangjun Pei ,
816 Qiang Xu1 , and Runqiu Huang. 2019b. Earthquake-induced chains of geologic hazards: Patterns, mechanisms,
817 and impacts. *Reviews of Geophysics*, 57, 421–503. <https://doi.org/10.1029/2018RG000626>
818
819 Farr, T. G., et al. (2007), The Shuttle Radar Topography Mission, *Rev. Geophys.*, 45, RG2004,
820 doi:10.1029/2005RG000183.
821
822 Fell, R., Corominas, J., Bonnard, C., Cascini, L., Leroi, E., & Savage, W. Z. 2008. Guidelines for landslide
823 susceptibility, hazard, and risk zoning for land use planning. *Engineering Geology*, 102(3–4), 85–98.
824 <https://doi.org/10.1016/j.enggeo.2008.03.022>

825 Francis, O. Fan, X., Hales, T., Hobley, D., Xu, Q., Huang, R (2022) ‘The fate of sediment after a large
826 earthquake’, *Journal of Geophysical Research: Earth Surface*, 127(3). doi:10.1029/2021jf006352

827 Gong, X.-L., Chen, X.-Q., Chen, K.-T., Zhao, W.-Y. and Chen, J.-G. 2021. Engineering planning method and
828 control modes for debris flow disasters in scenic areas. *Frontiers in earth science* 9. Available at:
829 <http://dx.doi.org/10.3389/feart.2021.712403>

830 Google Earth Pro. Version 9.189.0.0 “Location of Cutou gully, Chediguan Gully and Xiaojia Gully,
831 Sichuan, China”. Image taken 2020. Accessed June 2, 2023.

832 Guo, X., Cui, P., Li, Y., Ma, L., Ge, Y., and Mahoney, W.B. 2016. Intensity–duration threshold of rainfall-
833 triggered debris flows in the Wenchuan Earthquake affected area, China. *Geomorphology* (Amsterdam,
834 Netherlands) 253, pp. 208–216. Available at: <http://dx.doi.org/10.1016/j.geomorph.2015.10.009>.

835 Guzzetti, F. et al. 2008. The rainfall intensity-duration control of shallow landslides and debris flows: An
836 update. *Landslides* 5(1), pp. 3–17. Doi: [10.1007/s10346-007-0112-1](http://dx.doi.org/10.1007/s10346-007-0112-1).

837 Hao, P., Hooimeijer, P., Sliuzas, R and Geertma, S. 2013 ‘What drives the spatial development of urban villages
838 in China?’, *Urban Studies*, 50(16), pp. 3394–3411. doi:10.1177/0042098013484534

839 Hao, P. (2012) *Spatial evolution of urban villages in Shenzhen*. dissertation. University of Utrecht. Available at:
840 https://webapps.its.utwente.nl/librarywww/papers_2012/phd/puhao.pdf

841 He, N., Fu, Q., Zhong, W., Yang, Z., Cai, X. and Xu, L. 2022. Analysis of the formation mechanism of debris
842 flows after earthquakes – A case study of the Legugou debris flow. *Frontiers in ecology and evolution* 10.
843 Available at: <http://dx.doi.org/10.3389/fevo.2022.1053687>

844 Horton, A.J. et al. (2019) ‘Identifying post-earthquake debris flow hazard using Massflowx’, *Engineering*
845 *Geology*, 258, p. 105134. doi:10.1016/j.enggeo.2019.05.011

846 Hu, K.H., Cui, P., and Zhang, J.Q. 2012. Characteristics of damage to buildings by debris flows on 7 August
847 2010 in Zhouqu, Western China. *Natural hazards and earth system sciences* 12(7), pp. 2209–2217. Available
848 at: <https://nhess.copernicus.org/articles/12/2209/2012/nhess-12-2209-2012.pdf>.
849

850 Huang, R. Q., & Li, W. L. 2009. Analysis of the geo-hazards triggered by the 12 May 2008 Wenchuan
851 Earthquake, China. *Bulletin of Engineering Geology and the Environment*, 68(3), 363–371.
852 <https://doi.org/10.1007/s10064-009-0207-0>
853

854 Huang, R., Pei, X., Fan, X., Zhang, W., Li, S. and Li, B. 2012. The characteristics and failure mechanism of
855 the largest landslide triggered by the Wenchuan earthquake, May 12, 2008, China. *Landslides* 9(1), pp. 131–
856 142. Available at: <http://dx.doi.org/10.1007/s10346-011-0276-6>.
857

858 Huang, R. and Li, W. 2014. Post-earthquake landsliding and long-term impacts in the Wenchuan earthquake
859 area, China. *Engineering geology* 182, pp. 111–120. Available at:
860 <http://dx.doi.org/10.1016/j.enggeo.2014.07.008>.
861

862 Hübl, J. and Fiebigler, G. 2005. Chap. 18 - Debris-flow mitigation measures. In: *Debris-flow Hazards and*
863 *Related Phenomena*. Berlin, Heidelberg: Springer Berlin Heidelberg, pp. 445–487. Available at:
864 https://link.springer.com/content/pdf/10.1007/3-540-27129-5_18.pdf
865

866 Ivanov, P., Geological Institute, Bulgarian Academy of Sciences, Acad. Georgi Bonchev Str., Bl. 24, 1113
867 Sofia, Bulgaria, Dobrev, N., Berov, B., Frantzova, A., Krastanov, M., Nankin, R., Geological Institute,
868 Bulgarian Academy of Sciences, Acad. Georgi Bonchev Str., Bl. 24, 1113 Sofia, Bulgaria, & Geological
869 Institute, Bulgarian Academy of Sciences, Acad. Georgi Bonchev Str., Bl. 24, 1113 Sofia, Bulgaria. (2022).
870 Landslide risk for the territory of Bulgaria by administrative districts. *Geologica Balkanica*, 51(3), 21–28.
871 <https://doi.org/10.52321/geolbalt.51.3.21>
872

873 Iverson, R.M., Schilling, S.R. and Vallance, J.W., 1998, Objective delineation of areas at risk from inundation
874 by lahars: *Geological Society of America Bulletin*, V 110, no.8, p. 972-984.

875 Jiang, W., Deng, Y., Tang, Z., Cao, R., Chen, Z. and Jia, K. 2016. Adaptive capacity of mountainous rural
876 communities under restructuring to geological disasters: The case of Yunnan Province. *Journal of rural*
877 *studies* 47, pp. 622–629. Available at: <http://dx.doi.org/10.1016/j.jrurstud.2016.05.002>.

878 Kean, J.W. et al. 2019. Inundation, flow dynamics, and damage in the 9 January 2018 Montecito debris-flow
879 event, California, USA: Opportunities and challenges for post-wildfire risk assessment. *Geosphere* 15(4), pp.
880 1140–1163. Available at: <http://dx.doi.org/10.1130/ges02048.1>.

881 Li, C., Wang, M. and Liu, K. 2018. A decadal evolution of landslides and debris flows after the Wenchuan
882 earthquake. *Geomorphology (Amsterdam, Netherlands)* 323, pp. 1–12. Available at:
883 <http://dx.doi.org/10.1016/j.geomorph.2018.09.010>.

884 Li, N., Tang, C., Zhang, X., Chang, M., Shu, Z. and Bu, X. 2021b. Characteristics of the disastrous debris flow
885 of Chediguan gully in Yinxing town, Sichuan Province, on August 20, 2019. *Scientific reports* 11(1). Available
886 at: <https://www.nature.com/articles/s41598-021-03125-x>

887 Li, Y. et al. 2024. Assessment of debris flow risk in Mentougou District, Beijing, based on runoff of potential
888 debris flow. *Frontiers in earth science* 12. Available at: <http://dx.doi.org/10.3389/feart.2024.1426980>.

889 Liu, J., You, Y., Chen, X., Liu, J. and Chen, X. 2014. Characteristics and hazard prediction of large-scale
890 debris flow of Xiaojia Gully in Yingxiu Town, Sichuan Province, China. *Engineering geology* 180, pp. 55–67.
891 Available at: <https://www.sciencedirect.com/science/article/pii/S0013795214000702>

892 Liu, J., You, Y., Chen, X. and Chen, X. 2016. Mitigation planning based on the prediction of river blocking by
893 a typical large-scale debris flow in the Wenchuan earthquake area. *Landslides* 13(5), pp. 1231–1242. Available
894 at: <http://dx.doi.org/10.1007/s10346-015-0615-0>

895 Liu, J., Mason, P.J. and Bryant, E.C. 2018. Regional assessment of geohazard recovery eight years after the
896 Mw7.9 Wenchuan earthquake: a remote-sensing investigation of the Beichuan region. *International journal of*
897 *remote sensing* 39(6), pp. 1671–1695. Available at: <http://dx.doi.org/10.1080/01431161.2017.1410299>.

898 Luo, H.Y., Fan, R.L., Wang, H.J., and Zhang, L.M. 2020. Physics of building vulnerability to debris flows,
899 floods, and earth flows. *Engineering geology* 271(105611), p. 105611. Available at:
900 <https://www.sciencedirect.com/science/article/pii/S0013795219322227>.

901 Luo, H.Y., Zhang, L.M., Zhang, L.L., He, J., and Yin, K.S. 2023. Vulnerability of buildings to landslides: The
902 state of the art and future needs. *Earth-science reviews* 238(104329), p. 104329. Available at:
903 <https://www.sciencedirect.com/science/article/pii/S0012825223000181>.

904 Mattia Marconcini, Annkatrin Metz-Marconcini, Thomas Esch and Noel Gorelick. Understanding Current
905 Trends in Global Urbanisation - The World Settlement Footprint Suite. *GI_Forum* 2021, Issue 1, 33-38
906 (2021) <https://austriaca.at/0xc1aa5576%200x003c9b4c.pdf>

907 McGuire, L.A., Rengers, F.K., Kean, J.W. and Staley, D.M. 2017. Debris flow initiation by runoff in a recently
908 burned basin: Is grain-by-grain sediment bulking or en masse failure to blame?: DEBRIS FLOW
909 INITIATION. *Geophysical research letters* 44(14), pp. 7310–7319. Available at:
910 <http://dx.doi.org/10.1002/2017gl074243>.

911 OpenStreetMap contributors. OpenStreetMap database [PostgreSQL via API]. OpenStreetMap Foundation:
912 Cambridge, UK. 2024 [cited 20 Jul 2023]. © OpenStreetMap contributors. Available under the Open Database
913 Licence from: [openstreetmap.org](https://www.openstreetmap.org). Data mining by Overpass turbo. Available at <https://www.openstreetmap.org>

914 Papathoma-Köhle, M., Kappes, M., Keiler, M. and Glade, T. 2011. Physical vulnerability assessment for alpine
915 hazards: state of the art and future needs. *Natural hazards (Dordrecht, Netherlands)* 58(2), pp. 645–680.
916 Available at: <http://dx.doi.org/10.1007/s11069-010-9632-4>.

917 Peng, M., Zhang, L.M., Chang, D.S. and Shi, Z.M. 2014. Engineering risk mitigation measures for the landslide
918 dams induced by the 2008 Wenchuan earthquake. *Engineering geology* 180, pp. 68–84. Available at:
919 <https://www.sciencedirect.com/science/article/pii/S0013795214000696>.

920
921 Petley, D. 2023. *The 27 June 2023 landslide at Miansi, Sichuan Province, China*. Available at:
922 <https://blogs.agu.org/landslideblog/2023/06/29/miansi-landslide-1/>
923

924 Shen, P., Zhang, L. M., Chen, H. X., & Gao, L. (2017). Role of vegetation restoration in mitigating hillslope
925 erosion and debris flows. *Engineering Geology*, 216, 122–133. <https://doi.org/10.1016/j.enggeo.2016.11.019>

926 Shu, B., Chen, Y., Amani-Beni, M. and Zhang, R. 2022. Spatial distribution and influencing factors of
927 mountainous geological disasters in southwest China: A fine-scale multi-type assessment. *Frontiers in*
928 *environmental science* 10. Available at: <http://dx.doi.org/10.3389/fenvs.2022.1049333>.

929 Tang, C., Rengers, N., van Asch, T.W.J., Yang, Y.H. and Wang, G.F. 2011. Triggering conditions and
930 depositional characteristics of a disastrous debris flow event in Zhouqu city, Gansu Province, northwestern
931 China. *Natural hazards and earth system sciences* 11(11), pp. 2903–2912. Available at:
932 <https://nhess.copernicus.org/articles/11/2903/2011/nhess-11-2903-2011.pdf>.
933

934 Tang, C., Van Westen, C.J., Tanyas, H. and Jetten, V.G. 2016. Analysing post-earthquake landslide activity
935 using multi-temporal landslide inventories near the epicentral area of the 2008 Wenchuan earthquake. *Natural*
936 *hazards and earth system sciences* 16(12), pp. 2641–2655. Available at: [http://dx.doi.org/10.5194/nhess-16-](http://dx.doi.org/10.5194/nhess-16-2641-2016)
937 [2641-2016](http://dx.doi.org/10.5194/nhess-16-2641-2016).
938

939 Tang, Y. et al. 2022. Assessing debris flow risk at a catchment scale for an economic decision based on the
940 LiDAR DEM and numerical simulation. *Frontiers in earth science* 10. Available at:
941 <http://dx.doi.org/10.3389/feart.2022.821735>
942

943 Thouret, J.-C., Antoine, S., Magill, C. and Ollier, C. 2020. Lahars and debris flows: Characteristics and
944 impacts. *Earth-science reviews* 201(103003), p. 103003. Available at:
945 <http://dx.doi.org/10.1016/j.earscirev.2019.103003>.
946

947 Wang, C., Li, S. and Esaki, T. 2008. GIS-based two-dimensional numerical simulation of rainfall-induced
948 debris flow. Available at: <https://nhess.copernicus.org/articles/8/47/2008/nhess-8-47-2008.pdf>

949 Wei, L., Hu, K. and Liu, J. 2022. Automatic identification of buildings vulnerable to debris flows in Sichuan
950 Province, China, by GIS analysis and Deep Encoding Network methods. *Journal of flood risk*
951 *management* 15(4). Available at: <http://dx.doi.org/10.1111/jfr3.12830>

952 Wei, L., Hu, K., Liu, S., Ning, L., Zhang, X., Zhang, Q. and Rahim, M.A. 2024. The vulnerability of buildings
953 to a large-scale debris flow and outburst flood hazard cascade that occurred on 30 August 2020 in Ganluo,
954 southwest China. *Natural hazards and earth system sciences* 24(11), pp. 4179–4197. Available at:
955 <http://dx.doi.org/10.5194/nhess-24-4179-2024>.

956 Wei, L., Hu, K. and Liu, J. 2021 ‘Quantitative analysis of the debris flow societal risk to people inside buildings
957 at different times: A case study of Luomo Village, Sichuan, Southwest China’, *Frontiers in Earth Science*, 8.
958 doi:10.3389/feart.2020.627070.

959 Wei, L., Hu, K.-H. and Hu, X.-D. 2018. Rainfall occurrence and its relation to flood damage in China from
960 2000 to 2015. *Journal of mountain science* 15(11), pp. 2492–2504. Available at:
961 <http://dx.doi.org/10.1007/s11629-018-4931-4>

962 World Settlement Footprint Evolution data (1985-2015) ©DLR [cited Jul 2023]. 2019 All rights
963 reserved. <https://geoservice.dlr.de/web/maps/eoc/wsfevolution>
964

965 Wu, Y., Liu, X., Wang, J., Liu, L. and Shi, P. 2016. Landslide and debris flow disasters in China.
966 In: *IHDP/Future Earth-Integrated Risk Governance Project Series*. Berlin, Heidelberg: Springer Berlin
967 Heidelberg, pp. 73–101.
968

969 Yan, Y., Ge, Y.G., Zhang, J.Q. and Zeng, C. 2014. Research on the debris flow hazards in Cutou Gully,
970 Wenchuan County on July 10, 2013. *Journal of Catastrophology*, 29(3), pp.229-234.
971

972 Yang, Y., Tang, C., Tang, C., Chen, M., Cai, Y., Bu, X. and Liu, C. 2023. Spatial and temporal evolution of
973 long-term debris flow activity and the dynamic influence of condition factors in the Wenchuan earthquake-
974 affected area, Sichuan, China. *Geomorphology (Amsterdam, Netherlands)* 435(108755), p. 108755. Available
975 at: <http://dx.doi.org/10.1016/j.geomorph.2023.108755>.

976 Zeng, Q.L., Yue, Z.Q., Yang, Z.F. and Zhang, X.J. 2009. A case study of long-term field performance of
977 check-dams in mitigation of soil erosion in Jiangjia stream, China. *Environmental geology* 58(4), pp. 897–911.
978 Available at: <http://dx.doi.org/10.1007/s00254-008-1570-z>.

979 Zeng, C., Cui, P., Su, Z., Lei, Y. and Chen, R. 2015. Failure modes of reinforced concrete columns of buildings
980 under debris flow impact. *Landslides* 12(3), pp. 561–571. Available at: <http://dx.doi.org/10.1007/s10346-014-0490-0>
981

982 Zhang, S. 2014. Assessment of human risks posed by cascading landslides in the Wenchuan earthquake area.
983 (Hong Kong): Hong Kong University of Science and Technology.

984 Zhang, Z. and Li, Y. 2020. Coupling coordination and spatiotemporal dynamic evolution between urbanization
985 and geological hazards—A case study from China. *The Science of the total environment* 728(138825), p.
986 138825. Available at: <http://dx.doi.org/10.1016/j.scitotenv.2020.138825>.

987 Zhu, Cheng, Bao, Chen, and Huang 2022. Shaking table tests on the seismic response of slopes to near-fault
988 ground motion. *Geomechanics and engineering* 29(2), pp. 133–143. Available at:
989 <http://dx.doi.org/10.12989/gae.2022.29.2.133>.

Zou, Q., Cui, P., He, J., Lei, Y. and Li, S. 2019. Regional risk assessment of debris flows in China—An HRU-based approach. *Geomorphology* (Amsterdam, Netherlands) 340, pp. 84–102. Available at: <https://www.sciencedirect.com/science/article/pii/S0169555X19301849>

Statements & Declarations

Conflict of Interest

The authors disclose no financial or non-financial interests of competing interest during the preparation of this manuscript.

Author Contribution

All authors contributed to the study conception and design. Material preparation, data collection and analysis were performed by Isabelle Utley, Tristram Hales and Ekbal Hussain. The first draft of the manuscript was written by Isabelle Utley and all authors commented on previous versions of the manuscript. All authors read and approved the final manuscript